Renewable and Sustainable Energy Reviews 34 (2014) 20–29

Contents lists available at ScienceDirect

Renewable and Sustainable Energy Reviews

journal homepage: www.elsevier.com/locate/rser

Tower distortion and scatter factors of co-located wind speed sensors and turbulence intensity behavior

Shafiqur Rehman

Center for Engineering Research, Research Institute, King Fahd University of Petroleum and Minerals, Dhahran 31261, Saudi Arabia

A R T I C L E I N F O

Article history:
Received 18 August 2013
Received in revised form
2 February 2014
Accepted 1 March 2014
Available online 20 March 2014

Keywords:
Wind speed
Wind anemometer
Wind tower
Tower distortion factor
Scatter factor
Turbulence intensity
Wind power density

A B S T R A C T

The present study aims at evaluating the performance of wind speed sensors installed at different heights on a 40 m tall wind mast during a period of 33 months between July 01, 2006 and April 01, 2009. The performance has been evaluated by estimating the tower distortion factor (TDF), scatter factor (SCF), and studying the correlation ship between the co-located wind speed sensors. A total of 23,730 hourly mean wind speed records were used to evaluate each sensor. The overall values of TDF between wind speed sensors WS5/WS6 at 40 m and WS3/WS4 at 30 m were found to be 0.025 and 0.021 without tower shading and 0.047 and 0.035 with tower shading. The study showed that the performance of sensors did not deteriorate with time rather lower values of TDF were obtained with passage of time. At 40 m AGL for wind speed sensor WS5 the tower shading effect was pronounced (>1) within wind direction range of WD2 from 169° to 195° and in case of wind speed sensor WS6, the tower shading effect of <1 was evident from WD2 of 240° to 270°. More or less the same type of observations was noticed for wind speed sensors WS3 and WS4 at 30 m AGL. The SCF values were higher for wind speed sensor at 40 m compared to those at 30 m AGL.

Contents

1. Introduction

In this modern era of fast technological development and energy intensive life styles, the energy requirements are increasing tremendously on global, regional and national levels. Besides regular means of power production to meet these energy demands, new and renewable sources are being encouraged to supplement these requirements. Utilization of renewable sources of energy has two fold benefit, one it reduces the dependence on fossil fuels which means reduction in greenhouse gases (GHG) emissions and two to supply energy where there is no national or regional electrical grid. The fast developing and widely used sources of clean energy include the wind, solar thermal, solar photovoltaic (PV), hydro-, geothermal, and biomass. Of these sources of clean energy wind energy has been adapted by industries and accommodated by individual users due to its availability, ease of maintenance, low cost of operation and maintenance. The annual cumulative wind power installed capacity reached 282.587 GW in 2012 compared to 238.050 GW in 2011,

E-mail address: srehman@kfupm.edu.sa

http://dx.doi.org/10.1016/j.rser.2014.03.007
1364-0321/

Table 1
Details of the equipment installed at Juaymah.

S. no.	Item description	Technical information
1.	Symphonie internet enabled data logger	12 Channel, memory and remote data transfer facility, Symphonie GSM iPack kit
2.	Wind speed sensor, NRG#40 Three cup anemometer	Type: AC sine wave Accuracy: 0.1 m/s, range: 1–96 m/s Output: 0–125 Hz, threshold: 0.78 m/s
3.	Wind direction vane, NRG#200P	Type: potentiometer Accuracy: 1%, range: 360° mechanical Output: 0-Exc., voltage threshold: 1 m/s Dead band: max: 8° and typical 4°
4.	Temperature sensor #110S	Type: integrated circuit Accuracy: ±1.1 °C, range: −40 °C to 52.5 °C Output: 0–2.5 V DC Operating temperature range: −40 °C to 52.5 °C
5.	Pyranometer Li-Cor #LI-200SA	Type: global solar radiation Accuracy: 1%, range: 0–3000 W/m^2 Output: voltage DC Operating temperature range: −40 °C to 65 °C

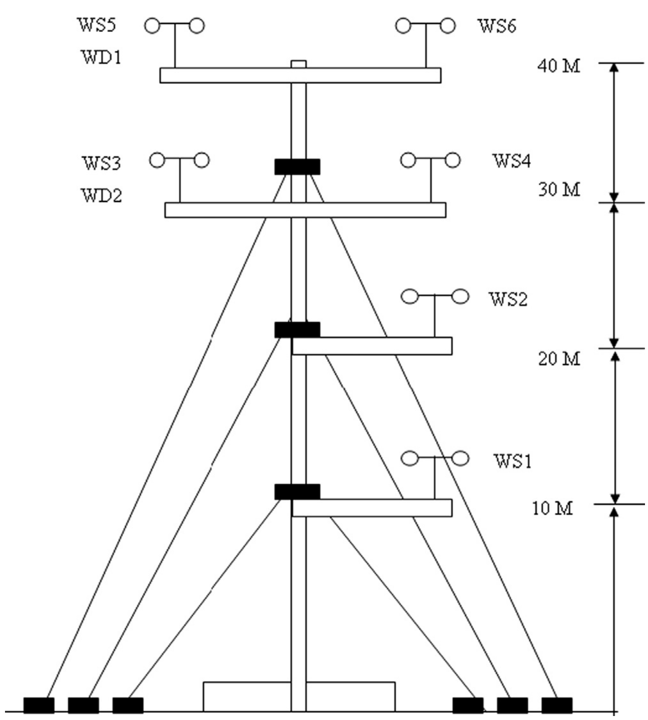


Fig. 1. Schematic diagram of placement of wind speed (WS) and wind direction (WD) sensors on 40 m tall wind mast.

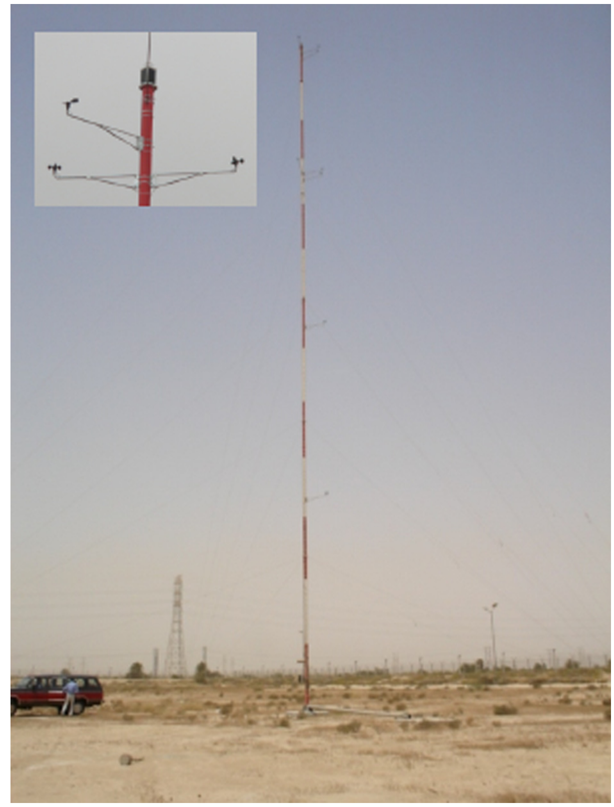


Fig. 2. Erected wind tower at Juaymah site.

an increase of 18.71%, Ref. [1]. With cumulative installed capacity of 75.324 GW, China remains the leader in wind power industry by the end of 2012. United States of America, Germany, Spain and India remained at 2nd, 3rd, 4th, and 5th place with total wind power installed capacities of 60.007 GW, 31.308 GW, 22.796 GW, and 18.421 GW, respectively by the end of 2012. With respect to new additions, USA remained on the top with 13.124 GW and China remained at the second place with 12.960 GW new wind power installations. However, Germany, India, and Spain remained at 3rd, 4th, and 5th, with new additional capacities of 2.415 GW, 2.336 GW, and 1.122 GW; respectively.

Wind power resource assessment is the key for effective and efficient wind power realization. Accurate wind resource assessment fully depends on the accuracy of the wind speed measurements. The wind speed measurements, though seems to be perfect, are affected by various inherent factors such as tower shading, sensor aging, power fluctuation, and dust accumulation effects. Of these, power fluctuation and dust accumulation effects are taken care by continuous monitoring and maintenance of the sensors but aging and shading effects need to be analyzed and taken care while conducting wind resource assessment. The local wind field is changed by a tower supporting an anemometer and also affects the readings of the anemometer. The impact of the tower on wind speed is most pronounced within the tower wake. The top mounted wind anemometers are least suffered from flow distortion caused by the tower and the protruded booms and hence provide the most accurate measurements, Lindelöw et al. [2]. However, in practice it becomes necessary to make measurements at lower heights for detailed wind shear information. This is usually carried out by installing cup anemometers on booms protruding from the tower. According to the IEC standard the influence on the wind speed measurement from the flow distortion induced by the tower must be kept below 1% and the influence from the boom should be below 0.5%, IEC-61400-12-1 [3]. Filippelli and Mackiewicz [4] reported larger than expected measurement deviations of cup anemometers mounted on tubular towers.

Canadillas et al. [5,6] carried out inter comparison between lidar and conventional mast-based instruments, such as cup/sonic and vanes based on 10-min averaged wind speed data and found good agreement between the two data sets with high correlation of more than 0.99 for all heights. Westerhellweg et al. [7] reported the assessment of the direction dependency of turbulence intensity in the German Bight. At the location of Fino1 a variation of turbulence intensity dependent on the wind direction was observed with higher turbulence intensity from north wind directions. The data at

Fino3 did not show such a distinct direction dependency. Wind turbulence significantly influences the fatigue loads acting on the wind turbines and high level of turbulence causes reduction in energy output and speeds-up the fatigue of the mechanical parts of wind turbine [8,9]. A value of TI of magnitude 0.10 or less is regarded as low level turbulence. A value of TI in the range of 0.10–0.25 is regarded as medium level turbulence while 0.25 or higher is considered as high level turbulence [8]. Kucukali and Dinçkal [10] carried out the turbulence analysis for wind data measured at 50 m above ground level in Izmitin, Turkey and found that turbulence intensity was negatively correlated with the normalized height from ground level with canopy height.

It is well understood and reported that the wind flow at 15 m is highly turbulent and the wind loads acting on collectors are significantly influenced by the characteristics of the approaching turbulent flow [11–13]. Sun et al. [14] presented an exhaustive review of the effects of wind loads on heliostats and trough collectors, considering wind flow characteristics, turbulence intensity, Reynolds number, the aspect ratio, porosity and mirror gap, wind loads on isolated collectors and on collector fields, and the effects of wind on beam quality.

Table 2
Tower distortion factors with and without tower shading at Juaymah wind mast site.

Year	Tower distortion factor				Records	
	No tower shading		With tower shading		Shading	
	WS5/WS6	WS3/WS4	WS5/WS6	WS3/WS4	No	Yes
All	0.025	0.021	0.047	0.035	21,200	24,108
2006	0.033	0.028	0.063	0.045	3894	4404
2007	0.029	0.022	0.048	0.036	7742	8760
2008	0.024	0.021	0.045	0.033	7587	8784
2009	0.019	0.020	0.033	0.035	1977	2160

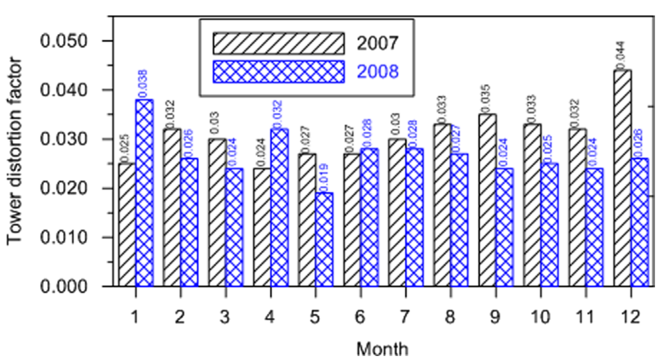


Fig. 3. Monthly variation of tower distortion factor at Juaymah wind mast site.

Saudi Arabia is a vast country with total land area of 2,149,690 km^2 and lies between latitudes 31 °N and 17.5 °N and longitudes 50 °E and 36.6 °E. The land elevation varies between 0 and 2600 m above the mean sea level (AMSL). Complex terrain is found in the southwest region of the Kingdom. The east and the west coasts of the Kingdom are located on the Arabian Gulf and Red Sea, respectively. Mainly two seasons, winter and summer, are observed during the year. Due to all these factors, it is difficult and economically infeasible to extend electric grid to all dwellings and communities spread over entire Saudi Arabian land. Moreover in Saudi Arabia, the per capita energy consumption has reached to 20 kWh/day in 2008 compared to 19.4 kWh/day in 2007, i.e. a net increase of 3.1% in just one year (Annual Report MOWE, 2008). A maximum of 10% increase in per capita energy was observed in year 2004 compared to that in 2003. On an average over 25 years period from 1984 to 2008, 4.1% annual increase in per capita energy per day has been observed, Ref. [15], which is really significant and needs to be addressed immediately. The overall increase in the generation capacity during the period 2004–2011 was 67.6%. The overall load growth during that period (2004–2011) was 73.7%; the growth in the load was the highest during the year 2006–2007 at 11.9%, followed by 10.8% during the year 2009–2010, Ref. [16].

The present study aims at understanding the effect of wind tower shading on the wind measurements, the aging effect of wind anemometers on wind measurements and lastly the variation of mean turbulence intensities at the wind measurement site. More such studies have become now necessary as Saudi Arabia is going ahead in big way to use renewable sources of energy to supplement its power sector. Furthermore, the recent King Abdullah City for Atomic and Renewable Energy (K.A.CARE) projections envision a total of 23,900 MW capacity of renewable power by 2020, increasing to 54,100 MW by 2032 has become a source of inspiration for scientists and engineers to enhance research efforts in different areas of renewable energy, Ref. [17].

2. Wind measurement description

The meteorological measurement equipment and sensors including wind speed, wind direction, ambient temperature, relative humidity, barometric pressure and global solar radiation were

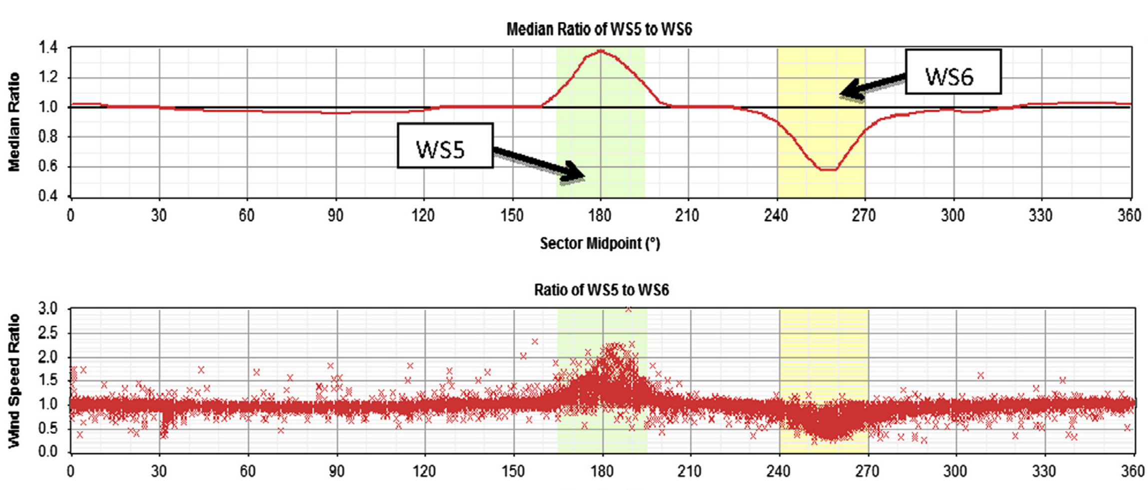


Fig. 4. Variation of wind speed ratio WS5/WS6 with wind direction at 40 m for entire data set.

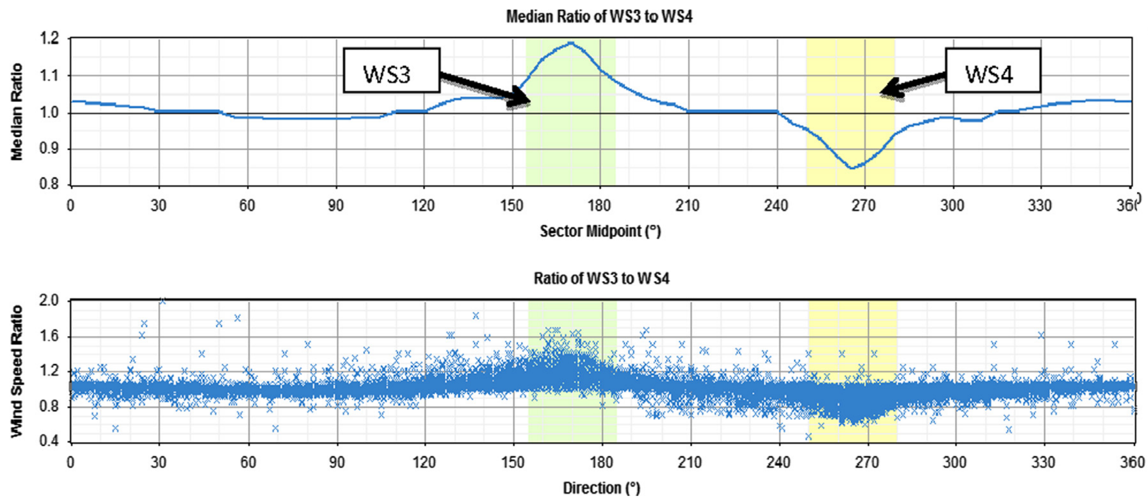


Fig. 5. Variation of wind speed ratio WS3/WS4 with wind direction at 30 m for entire data set.

Table 3
Scatter factors with and without tower shading at Juaymah wind mast site.

Year	Scatter factor				Records	
	No tower shading		With tower shading		Shading	
	WS5/WS6	WS3/WS4	WS5/WS6	WS3/WS4	No	Yes
All	0.049	0.045	0.065	0.052	20,937	24108
2006	0.047	0.043	0.065	0.049	3839	4404
2007	0.039	0.042	0.049	0.048	7634	8760
2008	0.048	0.038	0.065	0.046	7514	8784
2009	0.052	0.046	0.068	0.051	1950	2160

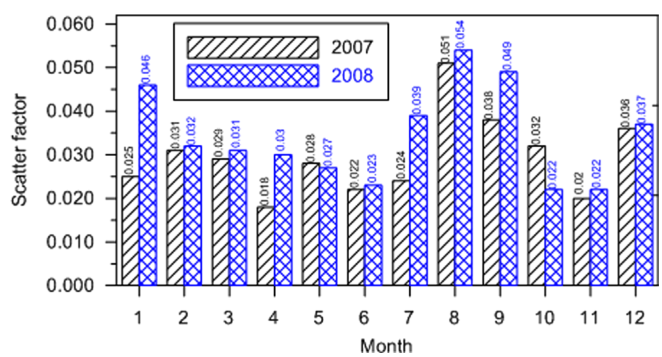


Fig. 6. Monthly variation of scatter factor at Juaymah wind mast site.

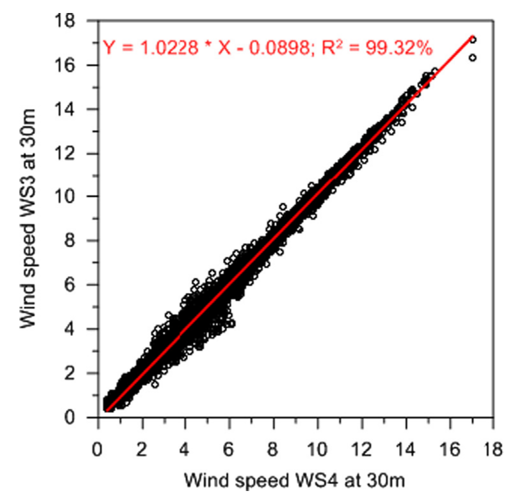


Fig. 7. Scatter plot between wind speeds WS3 and WS4 at 30 m for entire data set.

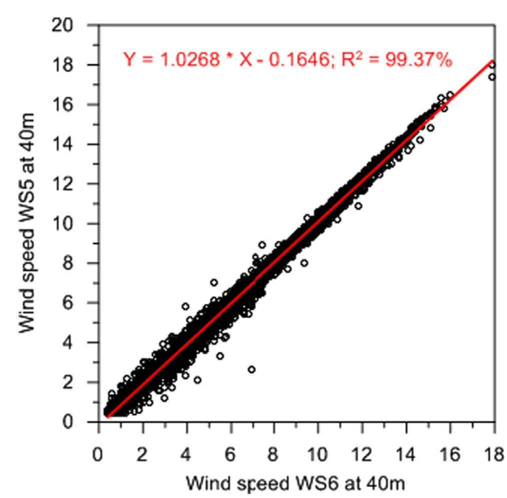


Fig. 8. Scatter plot between wind speeds WS5 and WS6 at 40 m for entire data set.

acquired from NRG, USA and installed at a power plant site in Juaymah (Latitude = 26°47.706′N, Longitude = 49°53.719′E, Altitude = 0 m) in eastern region of Saudi Arabia. The technical specifications and working ranges of all the sensors are provided in Table 1. The data collection site at Juaymah is an open area from all directions except a number of transmission line poles and cables. Data were recorded at every 10 min on a removable data storage card. The wind speed data were collected at 10, 20, 30, and 40 m height above the ground. At 10 and 20 m heights only one sensor was installed and the wind speed values were tagged as WS1 at 10 m and WS2 at 20 m above the ground level. At 30 and 40 m heights two sensors were installed and recorded data were tagged as WS3 and WS4 at 30 m, and WS5 and WS6 at 40 m. The wind direction data were recorded at 30 and 40 m as WD1 and WD2, respectively. A schematic diagram showing the positions of all the sensors on the mast is shown in Fig. 1. The actual wind mast installed at the site is shown in Fig. 2.

The surface air temperature (°C), and global solar radiation (W/m^2) data were also collected at 3 m above the ground surface. The raw data from the data acquisition system was transferred remotely via Al-Jawal GSM to the project office in Dhahran. The data received were further processed using NRG data logger software.

3. Tower distortion factor (TDF) estimation

Tower distortion refers to the change in the airflow caused by the presence of the meteorological tower on which the wind speed sensors are mounted. To detect and to minimize the worst effects of tower distortion, wind resource assessment is carried out by installing two wind speed sensors at each measurement height on a meteorological tower.

The tower distortion factor is the mean of the median ratios in each direction sector. A tower distortion factor of zero means that the sensors are always measuring the same wind speed in each sector. The larger the value of TDF means more overall difference between the readings of the two sensors. The TDF is calculated by finding the ratio of the two wind speeds in each time step, then binning those ratios by direction sector, finding their median value in each bin, and finally calculating the weighted mean of the departure of those median values from unity. The following equation defines the TDF, [18]:

$$\mathrm{TDF} = \frac{\sum_{i=1}^{n} |1-\eta_i| m_i}{\sum_{i=1}^{n} m_i} \quad (1)$$

where n is the number of wind director sectors which is taken as 72 in the present case, η_i is the median value of the ratios of wind speeds in direction sector i, and m_i is the number of records in direction sector i. The TDFs are calculated using Eq. (1) for data sets with tower shading and no tower shading and are summarized in Table 2. For entire data set the number of valid records with no shading were 21,200 and with shading 24,108, i.e. a difference of 2908 records between the two. For wind speed ratio WS5/WS6 the TDFs were 0.025 and 0.047 with no shading and with shading respectively, almost double value of TDF in case of tower shading effect compared to that without shading. At 30 m, TDFs were less than those at 40 m which simply means that tower shadow effect was more pronounced at 40 m than at 30 m. With passage of time, the values of TDF's were seen to be decreasing, as can be seen from Table 2, for TDF values of WS5/WS6 from year 2006 to 2008 under both shading and no shading scenarios. Similar type of changes was noticed in case of wind speed ratios at 30 m. This dictates that the performance of wind speed sensors did not deteriorate during the data collection period rather remained the same.

The monthly changes in TDF are shown in Fig. 3 for the years 2007 and 2008. As seen from this figure, no definite trend could be observed in TDF values during the years. The highest value of 0.038 and 0.044 were observed in January 2008 and December 2007. On the contrary, the minimum values of TDF of 0.019 and 0.024 were observed in the months of May and April during years 2008 and 2007, respectively.

For visual inspection of the tower shading patterns, two displays are used in the present case. To create these graphs, first the ratio of the wind speeds for each time step is calculated and then for the median ratio graph, the methodology sorted the ratios into 72 direction sector bins and calculated the median ratio in each sector bin. The tower distortion equation is based on median ratio values rather than mean ratio values because median values are less influenced by outliers. Wind speed data sets can include many erroneous wind speed values, which can lead to many spurious outlier values in the wind speed ratios. The highest and lowest values of the median ratios indicate the shaded sectors which are affected by the tower shading phenomenon.

At 40 m above ground level, the tower shading effect on wind speeds WS5 and WS6 for entire data set is shown in Fig. 4. In case of WS5 the tower shading effect is pronounced (>1) within wind direction range of WD2 from 169° to 200° as shown in Fig. 4. In case of WS6, the tower shading effect (<1) is evident from WD2 of 240° to 270°. These tower shading effects on WS5 and WS6 are also shown by scatter diagram of wind speed ratios versus wind direction WD2 in Fig. 4. Furthermore, for individual year data sets, the tower shading effect is pronounced (>1) within wind direction range of WD2 from 160° to 200° in 2007 and within WD2 range of 165° to 200° in 2008 for WS5. In case of WS6 the tower shading factor was <1 and the corresponding ranges of WD2 were 240–270 for both the years. The individual year values of wind direction ranges which had pronounced effect of tower shading were in almost the same ranges compared to those for entire data set.

For wind speeds at 30 m (WS3 and WS4), the tower shading effect is shown in Fig. 5. In case of WS3 the tower shading effect is pronounced (>1) within the wind direction range of WD1 from 155° to 185° as shown in Fig. 5. In case of WS4, the tower shading effect (<1) is evident from WD1 of 250° to 280°. These tower shading effects on WS3 and WS4 are also shown by scatter diagram of wind speed ratios versus wind direction WD1 in Fig. 5. The corrective measures can be taken by flagging the values of wind speed lying in the wind direction ranges as mentioned above.

4. Scatter factor (SCF) estimation

The scatter factor (SCF) is a measure of spread in the ratio of the readings of pair of wind speed sensors. It is calculated as a

Table 4
Best fit equations and coefficient of performance for scatter plots at 30 m and 40 m heights without tower shading.

Data	WS3/WS4	R^2	WS5/WS6	R^2
All	$Y=1.0288\,X-0.0898$	99.32	$Y=1.0268\,X-0.1646$	99.37
2007	$Y=1.0281\,X-0.0979$	99.33	$Y=1.0317\,X-0.1648$	99.36
2008	$Y=1.0253\,X-0.1354$	99.28	$Y=1.0269\,X-0.1852$	99.48

Table 5
Best fit equations and coefficient of performance for scatter plots at 30 m and 40 m heights with tower shading.

Data	WS3/WS4	R^2	WS5/WS6	R^2
All	$Y=1.0225\,X-0.1099$	98.38	$Y=1.0197\,X-0.1541$	96.21
2007	$Y=1.0291\,X-0.1336$	98.32	$Y=1.0263\,X-0.1809$	96.16
2008	$Y=1.0245\,X-0.1496$	98.43	$Y=1.0171\,X-0.1507$	96.15

Table 6
Annual mean turbulence intensity at different heights and in different years.

Data	All				2007				2008			
Description	WS3	WS4	WS5	WS6	WS3	WS4	WS5	WS6	WS3	WS4	WS5	WS6
Records in 15 m/s bin	23	16	36	28	3	0	5	4	13	11	22	16
Mean TI at 15 m/s	0.116	0.113	0.108	0.122	0.105	0	0.102	0.105	0.117	0.113	0.110	0.120
Representative TI at 15 m/s	0.126	0.122	0.122	0.117	0.117	0	0.124	0.127	0.126	0.121	0.120	0.115
IEC3 turbulence category	C	C	C	C	C	C	C	C	C	C	C	C

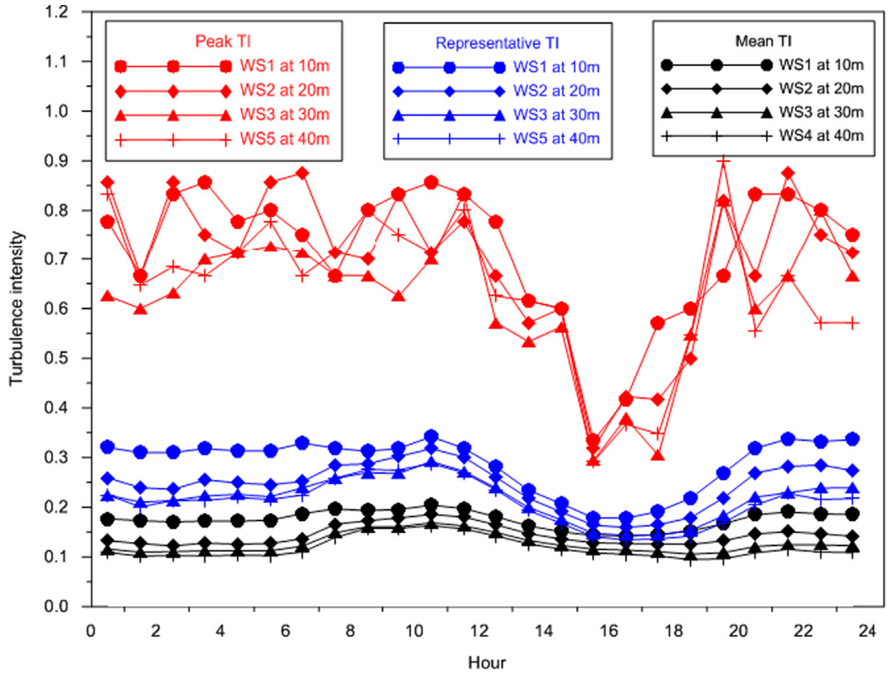


Fig. 9. Diurnal variation of turbulence intensity at different heights at Juaymah meteorological station.

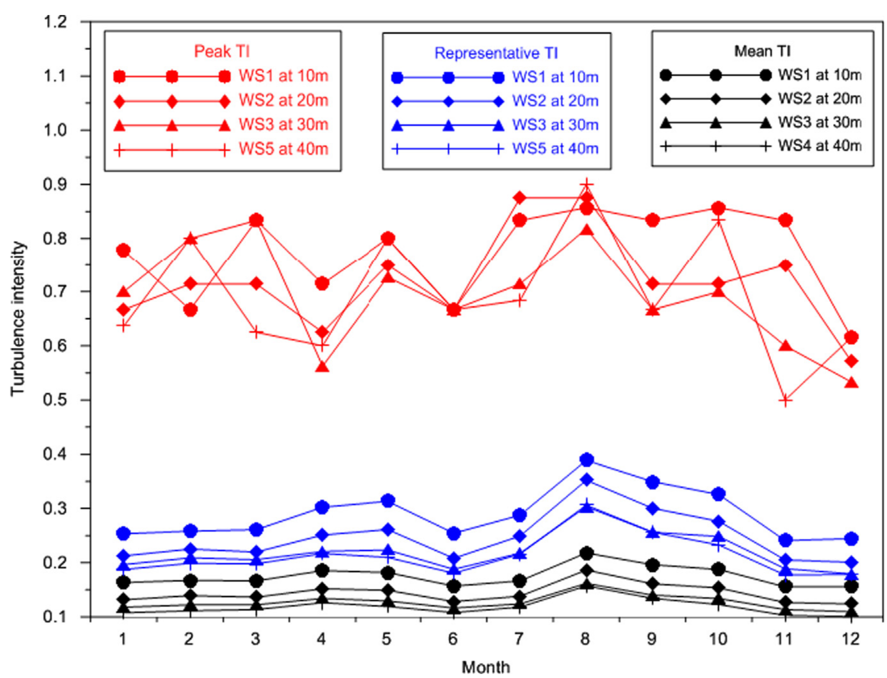


Fig. 10. Monthly variation of turbulence intensity at different heights at Juaymah meteorological station.

weighted mean of the standard deviation of the ratios in each direction sector. The mean is weighted by the number of data points in each sector. The following equation defines the scatter factor:

$$SCF = \frac{\sum_{i=1}^{n} \sigma_i m_i}{\sum_{i=1}^{n} m_i} \quad (2)$$

where n is the number of direction sectors, σ_i is the standard deviation of the ratios in direction sector i, and m_i is the number of records in direction sector i. The scatter factor is the weighted mean of the standard deviations measured in each direction sector. In the present case, the scatter factors are calculated using above Eq. (2) for co-located wind speed sensors at 30 m (WS3/WS4) and 40 m (WS5/WS6) heights at Juaymah meteorological station and are summarized in Table 3. It is obvious from Table 2 that SCF values are higher with tower shading effect compared to that without tower shading effect. The monthly mean values of SCF were found relatively higher in January, July, August, September and December months during the year while smaller during rest of the months as shown in Fig. 6. The highest values of 0.051 and 0.054 were found in the month of August corresponding to years 2007 and 2008, respectively. In general higher values of SCF were observed in 2008 compared to those in 2007, as can be seen from Fig. 6.

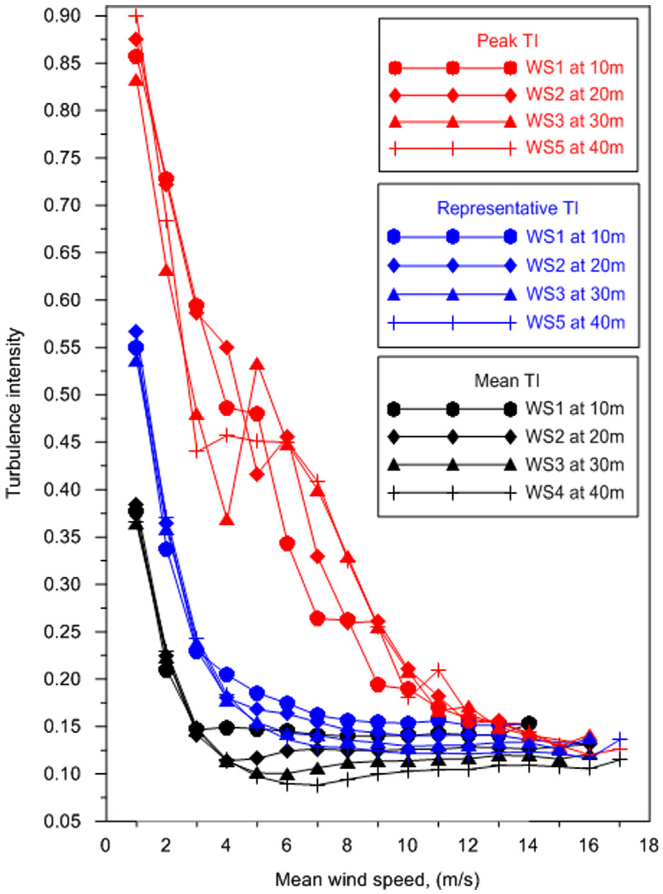


Fig. 11. Variation of turbulence intensity with wind speed at different heights at Juaymah meteorological station.

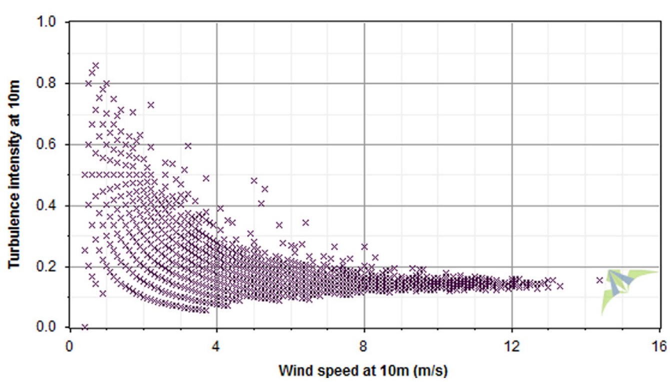


Fig. 12. Variation TI values with 10 min average wind speed at 10 m.

5. Correlation between co-located wind speed sensors

This section is devoted to the development of linear correaltions between co-located wind speed sensors at 30 and 40 m heights with and without tower shading effects. The scatter plot between wind speeds WS3 and WS4 at 30 m for entire data set duirng July 2006–March 2009 without tower shading is shown in Fig. 7. The best fit linear line is also drawn and has a coefficient of variation 99.32% which shows a high degree of correlation between the wind speeds measured at 30 m. Similarly, the scatter digram between the wind speeds WS5 and WS6 at 40 m shows a correlation coefficient of 99.37%, as shown in Fig. 8. The correlations between wind speed sensors at 30 and 40 m heights without tower shading effects are summarized in Table 4. The correlation coefficients' values were always more than 99% as can be seen

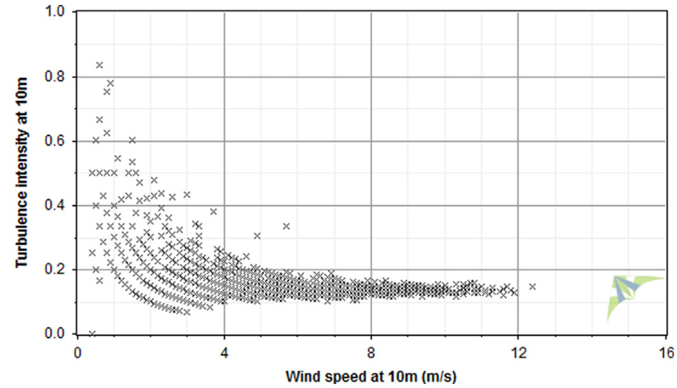


Fig. 13. Variation TI values with 10 min average wind speed at 10 m in wind direction bin 348.75–11.25°

from Table 4. The correlation coefficients for data set with tower shading effects were slighly less than those without tower shading, as can be observed from values summarized in Table 5. With tower shading effect, the correlation performance of the wind speed sensors at 30 m deteriorated by 1% while by 3% at 40 m, as can be seen from data given in Tables 4 and 5.

6. Turbulence intensity (TI) estimation

The turbulence intensity is a dimensionless number defined as the standard deviation of the wind speed within a time step divided by the mean wind speed over that time step. It is important in the classification of the site according to the International Electro-technical Commission (IEC). It is a measure of the gustiness of a wind resource. Lower turbulence results in lower mechanical loads on a wind turbine and vice versa. The turbulence intensity is calculated for each time step (10 min in the present case) using the following equation [19–21]:

$$\mathrm{TI} = \sigma_i / v_i \tag{3}$$

where v_i is the average wind speed in time step i and σ_i is the standard deviation of the wind speed within time step i (same unit as v_i).

The scatter plot of the turbulence intensity versus the wind speed shows a typical phenomenon; the highest values of turbulence intensity tend to correspond to the lowest wind speeds. The mean and representative TI values at 15 m/s wind speed along with IEC3 turbulence category for entire data set and individual years are given in Table 6 for Juaymah meteorological station. This table also included the number of records for which the wind speed was 15 m/s. The annual mean values of TI values at 15 m/s wind speed at 30 m were 0.116 and 0.113 corresponding to wind speed sensors WS3 and WS4, while at 40 m these values were 0.108 and 0.122 corresponding to wind speed sensors WS5 and WS6. Relatively smaller values of mean TI were observed during 2007 compared to those in 2008, as can be seen from Table 6. Usually, the mean TI values were smaller than the representative values of TI at 15 m/s wind speed. Raichle and Carson [19] reported annual average values of TI's below 0.17 at various sites in United States which shows that the present values of mean TI are compatible. Al-Yahyai et al. [20] analyzed the wind speed data measured at various locations in Oman and reported mean annual values of turbulence intensities as between 0.41 and 0.90 which are much higher than the one found in the present case.

The hourly and monthly mean values of TI calculated using the mean wind speeds and corresponding standard deviation at 10, 20, 30, and 40 above ground level are shown in Figs. 9 and 10,

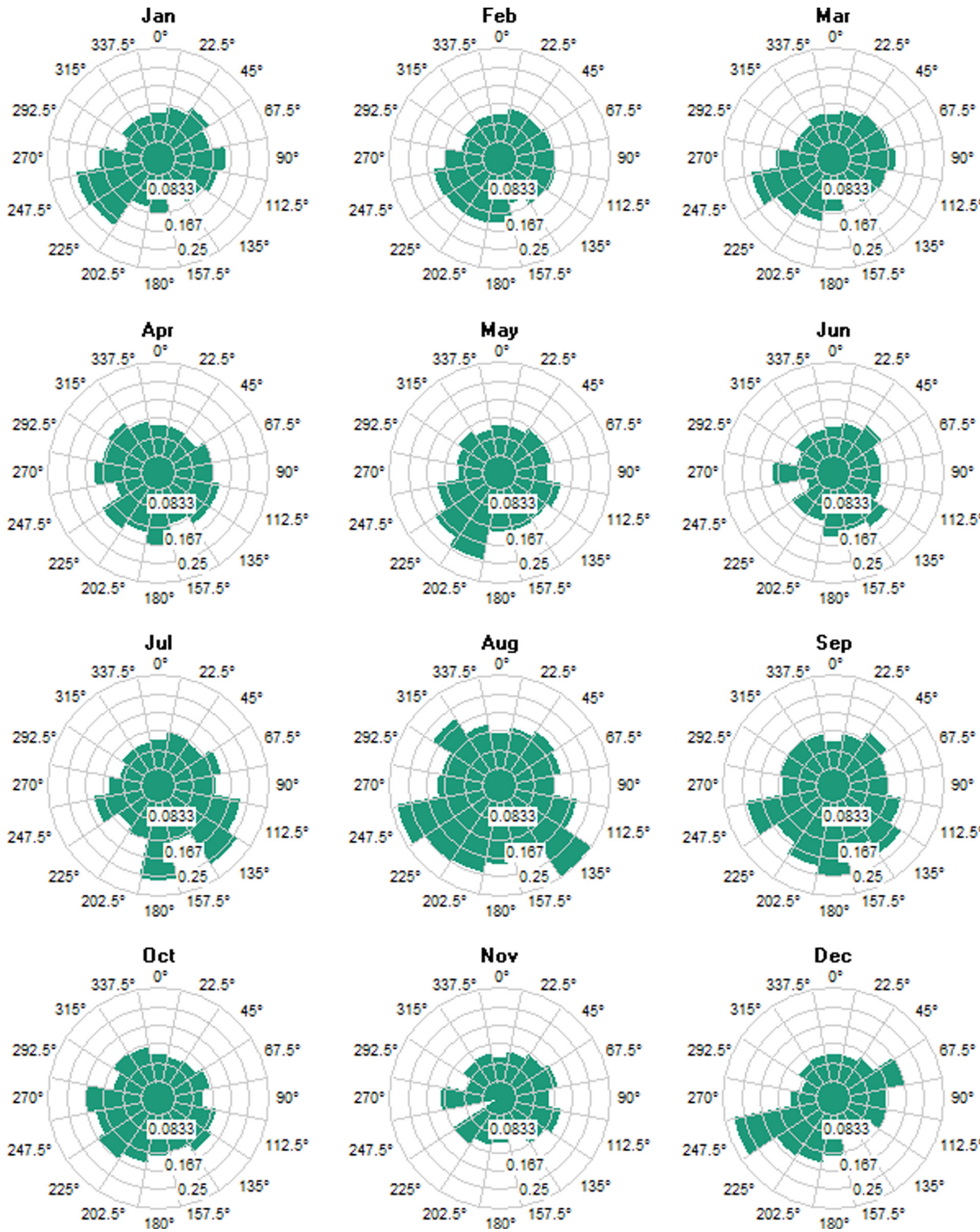


Fig. 14. Seasonal and sectorial variations of mean turbulence intensity at Juaymah.

respectively. The peak and representative values of TI are also included in these figures. Relatively smaller values of TI are observed during 14:00–19:00 compared to rest of the day, as can be seen from Fig. 9. Dahmouni et al. [21] reported higher values of TI during the period from midnight to 10:00 and lower during remaining period which is comparable with the present case. Al-Yahyai et al. [20] found minimum seasonal turbulence intensity of 0.33 at Qayroon Hyriti during summer and maximum seasonal intensity of 1.1 at Nizwa during winter.

As expected, the peak values of TI are highest at all the measurement heights followed by representative values of TI and exhibit almost the same diurnal trends as the mean TI. Moreover, the higher values of TI's were observed at lower heights compared to those at higher heights, as indicated by TI values in

Figs. 9 and 10. The mean TI values were always <0.15 at 40 m above ground level and <0.2 at 10 m. From monthly mean values of TI, it was noted that higher values of mean and representative TI's were observed during April–May and August–September while smaller during rest of the months. The mean TI values were always <0.15 at 40 m and <0.2 at 10 m above ground level, as can be seen from Fig. 10. Practically, as observed from Fig. 8, no definite seasonal trend could be obtained in the mean values of TI at Juaymah meteorological station. Similar types of observations were reported by Raichle and Carson [19] for various locations in United States. It was also noted that mean TI values at 15 m/s wind speed were always less than the reference and peak TI values at all the measurement heights and hence indicate no concerns for wind energy exploitation according to the 3rd edition of the IEC 61400-1.

The variation of mean TI, representative TI and peak TI values with mean wind speed is shown in Fig. 11. It is evident from these values that mean TI values are always less than the peak and representative TI values. It is also obvious that higher values of TI's were found at lower mean wind speed values. In particular the mean TI values were always <0.15 at all measurement heights at wind speed >4 m/s, as can be seen from Fig. 11. Moreover the TI values were found to be decreasing with increasing wind measurement heights.

The scatter diagram of TI with 10 min average wind speed is shown in Fig. 12 at 10 m. It is evident from this scatter diagram that the highest TI corresponds to the lowest wind speed. The scatter diagram of TI values at 10 m is found to be different in wind direction bin 348.75–11.25 (Fig. 13) than the one for all sectors (Fig. 12). It can be pointed out from TI values shown in Fig. 13 that the turbulence is always <0.2 in the targeted region i.e. region with wind speed >3.5 m/s which is usually the cut-in-wind speed of all the wind turbines. Durisic and Mikulovic [22] studied the turbulence characteristics of wind regime in the village Bavaniste in Srbia and found that the targeted region could be characterized by a low level of wind turbulence, amounting only 8.1% at the height of 60 m, which is favorable in so far as the efficiency and mechanical load of the perspective wind turbines in that region was concerned. The seasonal change in mean TI values corresponding to changing wind direction is shown in polar diagram (Fig. 14).

7. Conclusions

The present work utilized hourly mean wind speed data measured at different heights at Juaymah meteorological station in Saudi Arabia during July 01, 2006 and April 01, 2009 to study the performance of wind speed sensors with passage of time considering the tower distortion factor and the scatter factor. The findings of the study could be summarized as follows:

- AT 40 m above ground level (AGL) without tower shading effect the TDF decreased from 0.033 to 0.029 to 0.024 to 0.019 corresponding to 2006, 2007, 2008, and 2009, respectively. A similar trend was obtained for data set at 30 m AGL. Higher values of TDF were obtained for the case of tower shading effect. Furthermore, higher values of TDF were obtained for co-located sensors at 40 m compared to those at 30 m AGL.
- The monthly mean values of TDF showed higher values in winter time and relatively lower in summer for both the years 2007 and 2008.
- The scatter factors at 40 m with and without tower shading factor effect were 0.065 and 0.049 while at 30 m these values were 0.052 and 0.045. Higher values of SCF were observed at 40 m compared to those at 30 m. Furthermore, the values of SCF increased from 0.049 in 2007 to 0.065 in 2008 between wind speed sensors WS5/WS6 at 40 m and from 0.039 to 0.048 with and without tower shading effect.
- Truly speaking, no definite seasonal changes could be identified in the values of SCF during the years 2007 and 2008. The highest values of 0.051 and 0.054 were found in the month of August for both years respectively and lowest of 0.018 in 2007 and 0.022 in October and November 2008.
- The correlations between co-located wind speed sensors at 30 and 40 m AGL were excellent with R^2 values of $>99.3\%$ without tower shading effect and >98.3 with tower shading effect.
- The annual mean values of TI at 15 m/s wind speed at 30 m were 0.116 and 0.113 corresponding to wind speed sensors WS3 and WS4, while at 40 m these values were 0.108 and 0.122 corresponding to wind speed sensors WS5 and WS6.
- Relatively smaller values of mean TI were observed during 2007 compared to those in 2008.
- Smaller values of TI are observed during 14:00–19:00 compared to rest of the day.

Acknowledgment

The authors wish to acknowledge the support of the Research Institute of King Fahd University of Petroleum and Minerals, Dhahran, Saudi Arabia.

References

[1] Global Wind Energy Council (GWEC) annual report; 2012, ⟨http://www.gwec.net/global-figures/graphs/⟩ (accessed 13.08.1313).
[2] Lindelöw-Marsden P, Pedersen TF, Gottschall J, Vesth A, Paulsen RWU, Courtney MS. Flow distortion on boom mounted cup anemometers. Risø-R-1738(EN); August 2010.
[3] IEC 61400-12-1. Wind turbines—Part 12-1: power performance measurements of electricity producing wind turbines; 2005.
[4] Filippelli M, Mackiewicz, P. Experimental and computational investigation of flow distortion around a tubular meteorological mast. In: Proceedings of the CanWEA conference; 2005.
[5] Canadillas B, Westerhellweg A, Neumann T. Testing the performance of a ground-based wind LiDAR system—one year inter-comparison at the offshore platform Fino1. DEWI Mag 2011;38:58–64.
[6] Canadillas B, Begue A, Neumann T. Comparison of turbulence spectra derived from LiDAR and sonic measurements at the offshore platform FINO1. In: Proceedings of 10th German wind energy conference (DEWEK 2010). Bremen, Germany; November 17–18, 2010.
[7] Westerhellweg A, Canadillas B, Neumann T. Direction dependency of offshore turbulence intensity in the German Bight. DEWI Mag 2011;38:66–70.
[8] Jain P. Wind energy engineering. United States of America: McGraw Hill; 2011.
[9] Vestas: Vestas Brochures; 2012, ⟨http://www.vestas.com/en/media/brochures.aspx⟩.
[10] Kucukali S, Dinçkal Ç. Wind energy resource assessment of Izmitin the West Black Sea Coastal Region of Turkey. Renew Sustain Energy Rev 2012;30:790–5.
[11] Peterka JA, Derickson RG. Wind load design methods for ground based heliostats and parabolic dish collectors [Technical report for Sandia Laboratories, Report No. SAND92-7009]. 1992.
[12] Wu ZY, Gong B, Wang ZF. An experimental and numerical study of the gap effect on wind load on heliostat. Renew Energy 2009;35(4):797–806.
[13] Gong B, Wang ZF, Li ZN. Field measurements of boundary layer wind characteristics and wind loads of a parabolic trough solar collector. Sol Energy 2012;86:1880–98.
[14] Sun H, Gong B, Yao Q. A review of wind loads on heliostats and trough collectors. Renew Sustain Energy Rev 2014;32:206–21.
[15] MOWE. Electricity growth and development in the Kingdom of Saudi Arabia 1428–1429 H/2008 G. Ministry of Water and Electricity; 2008.
[16] MOWE. Annual Report 1432–1433 H/2011G. Kingdom of Saudi Arabia: Ministry of Water and Electricity (MOWE); 2011.
[17] Proposed competitive procurement process for the renewable energy program. Prepared by King Abdullah City for Atomic and Renewable Energy; 2013, ⟨http://www.kacare.gov.sa/cpp/sites/default/files/K.A.CARE%20Proposed%20Competitive%20Procurement%20Process%20for%20the%20Renewable%20Energy%20Program%20-%202013.pdf⟩.
[18] Wind Energy Reference Manual at www.windpower.org; 2013 (accessed 15.07.13).

[19] Raichle BW, Carson WR. Wind resource assessment of the Southern Appalachian Ridges in the Southeastern United States. Renew Sustain Energy Rev 2009;13:1104–10.
[20] Al-Yahyai S, Charabi Y, Gastli A, Al-Alawi S. Assessment of wind energy potential locations in Oman using data from existing weather stations. Renew Sustain Energy Rev 2010;14:1428–36.
[21] Dahmouni AW, Ben Salah M, Askri F, Kerkeni C, Ben Nasrallah S. Wind energy in the Gulf of Tunis, Tunisia. Renew Sustain Energy Rev 2010;14:1303–11.
[22] Durisic Z, Mikulovic J. Assessment of the wind energy resource in the South Banat region, Serbia. Renew Sustain Energy Rev 2012;16:3014–23.